Available online at www.sciencedirect.com

ScienceDirect

journal homepage: www.elsevier.com/locate/he

Effect of hydrogen enrichment on the auto-ignition of lean *n*-pentane/Hydrogen mixtures at elevated pressure

Xue Jiang[*], *Fuquan Deng*, *Youshun Pan*, *Wuchuan Sun*, *Zuohua Huang*

State Key Laboratory of Multiphase Flows in Power Engineering, Xi'an Jiaotong University, Xi'an 710049, People's Republic of China

HIGHLIGHTS

- New ignition delay time data of hydrogen/*n*-pentane/O_2/Ar mixtures were provided.
- Hydrogen doping can nonlinearly promote the auto-ignition of *n*-pentane.
- The binary mixture exhibits the *n*-pentane like activation energy.
- Hydrogen addition can promote the H-abstractions of the *n*-pentane.

ARTICLE INFO

Article history:
Received 14 April 2020
Received in revised form
17 July 2020
Accepted 2 August 2020
Available online 24 August 2020

Keywords:
Hydrogen
n-Pentane
Ignition delay
Chemical kinetic
Fuel blending

ABSTRACT

To understand the synergistic effect of hydrogen-enriched combustion of hydrocarbons in the high temperatures, ignition delay times of lean ($\varphi = 0.5$) *n*-pentane/hydrogen mixtures with various hydrogen volumetric contents ($X_{H2} = 0$–95%) were measured in a shock tube at pressures of 2, 10 and 20 atm. As expected, the ignition delay time of *n*-pentane is decreased when doping with hydrogen. Interestingly, the effect of hydrogen addition on auto-ignition is nonlinear. Note that even the hydrogen proportion is as large as 95%, the ignition delay time of the binary mixture exhibits the *n*-pentane-like activation energy and pressure dependence characteristics. Reasons for the above-mentioned behaviors were analyzed.

© 2020 Hydrogen Energy Publications LLC. Published by Elsevier Ltd. All rights reserved.

Introduction

In recent years, energy and environmental issues are forcing people to look for clean alternative fuels of petroleum and develop advanced engine technologies. Hydrogen is considered as a promising energy source of the future. It is commonly produced from the hydrogen-containing material, such as methane, methanol, gasoline, ammonia, and water [1], besides, it also can be produced from solar, wind, biomass and nuclear energy [2]. The most noteworthy feature of hydrogen is carbon-free, which can be used as clean and non-pollution alternative fuel for engines. Hydrogen was also characterized with broad flammability limit and high flame

* *Corresponding author.*
E-mail address: xuejiang1128@xjtu.edu.cn (X. Jiang).
https://doi.org/10.1016/j.ijhydene.2020.08.004
0360-3199/© 2020 Hydrogen Energy Publications LLC. Published by Elsevier Ltd. All rights reserved.

speed during combustion [3–7]. Even with the advantages above, many problems such as backfire, reduction in the power output, etc., restrict the use of pure hydrogen in combustion devices [2,8]. Therefore, hydrogen is more preferred to be used by blending with other fuels in engine applications. As an additive, hydrogen provides possibilities to realize lean-burn in engine application thus result in extremely low emissions and high efficiency. It is found that by adding hydrogen to the hydrocarbon fueled industrial gas turbine, the NOx emission can be largely reduced [9], suggesting that power plants have the potential to achieve lower emission by using hydrogen-enriched fuel [2,9]. Researches also showed that when using natural gas-hydrogen dual fuel in gas turbines, the backfire phenomenon of hydrogen can be inhibited by natural gas addition, in the meantime, blending hydrogen into natural gas can effectively extend the lean burn limit in the engine operation to avoid misfire [8].

The implementation of hydrogen enrichment strategies in engines must rely on a comprehensive understanding of the combustion chemistry of both individual fuels and their synergistic effects. The combustion characteristics and chemical kinetics of hydrogen-enriched methane have been studied extensively. The laminar burning velocities of hydrogen/methane blends have been studied experimentally and numerically in Refs. [5,10–16]. In general, these studies found that the laminar burning velocities were promoted as the hydrogen blending ratio increases, indicating that hydrogen enrichment can promote the reactivity of the laminar premixed combustion of methane. Note that the promotion effect becomes obvious when the hydrogen content is relatively large, saying that more than 40%. The oxidation of hydrogen/methane and/or hydrogen/natural gas blends have been studied in the jet-stirred reactors [17,18], indeed, the fuel consumption was accelerated by hydrogen enrichment, besides, the production of the stable intermediate species was also promoted. The hydrogen enrichment was also found to decrease the auto-ignition delays of methane in the high temperature shock tube conditions [19–22] and the low to intermediate temperature rapid compression machine conditions [23,24]. In addition, several studies have been conducted to understand the ignition delay characteristics of hydrogen-enriched light alkanes (C1–C4) blends [4,19–23,25–29], however, there is not much research focusing on hydrogen blending with heavier alkanes.

n-Pentane is known as the transition between the liquid and gaseous alkanes, the fundamental research of which has attracted much attention, especially in recent years. It is recognized as a constituent for liquid natural gas and petrol [30]. Besides, the combustion chemistry of *n*-pentane can be served as a reference to understand the chemical kinetics of heavier alkanes. The macroscopic ignition delay property of *n*-pentane measured by the shock tube and RCM were reported in Refs. [31–33] from different research groups. The experimental data cover a wide range of pressure from 1 to 530 atm, from lean to rich conditions (φ = 0.3 to 2.0.), and from high to low temperatures (643–1718 K). Laminar combustion characteristics of *n*-pentane were also reported in previous publications [34–36]. JSR experiments were conducted in Refs. [37,38] which successfully identified the microscopic speciation of *n*-pentane oxidation.

Ignition delay time data are valuable for the development of the chemical kinetic model, however, to the best of the author's knowledge, the ignition delay time of hydrogen/*n*-pentane binary mixture which indicating the kinetic interactions of dual fuels, have not yet been reported. In order to guide the practical application, to improve the dual-fuel kinetic model, and to deeply understand the chemical kinetic influence of the hydrogen enrichment, the auto-ignition delays of hydrogen/*n*-pentane mixtures were measured using a shock tube at various hydrogen addition level and elevated pressures. The performances of several representative kinetic models were tested against our experimental data. In addition, we explored the influences of pressure and hydrogen addition on the auto-ignition of the hydrogen/*n*-pentane binary mixtures based on the observed experimental phenomena and interpret the changing kinetic to obtain a deeper understanding of hydrogen-enriched combustion.

Experiment and simulation

SHOCK tube experiment

A shock tube apparatus with double diaphragms design was used to determine the ignition delay times. Details of the experimental setup, device performance verification and experimental error evaluation are given in earlier Refs. [19,39,40]. Briefly, this shock tube has a 4 m long driver section and a 4.8 m long driven section, with a diameter of 115 mm. To determine the incident shock velocity, four fast-response pressure transducers (PCB 113B26) were installed at fixed intervals along the end of the driven section. The time when the shock wave reaches each pressure transducer position is recorded by time counters (FLUKE, PM6690). In the experiment, OH* chemiluminescencel was detected by a photomultiplier mounted on the shock tube end wall. The onset of ignition is defined according to the extrapolation at the steepest slope of the OH* emission trace to the baseline. The ignition delay time is considered as the interval between the arrival time of the reflected shock and the onset of ignition, as indicated in Fig. 1. The typical attenuation rates of incident shock (dp/Pdt) is 4.2%/ms. The uncertainties of the measured ignition delay time were estimated to be ±20%.

In this experiment, "air" is made up of oxygen and argon with the proportion of 21:79. All the test fuel/"air" mixtures were diluted by 80% argon. The purities of hydrogen, oxygen, and argon are higher than 99.999%, and purity of *n*-pentane is 99.5%. The helium/nitrogen mixture is used as the driver gas. The test mixtures were prepared in a 128 L stainless steel tank according to the partial pressure of each gas component. The test mixture compositions are given in Table 1.

Numerical simulation

Simulation of the ignition delay time was performed using the SENKIN code [42] in the CHEMKIN II program [43] based on the zero-dimensional and constant volume adiabatic model. The computational ignition delay time is determined according to the simulated OH* emission. The pressure rise due to the non-

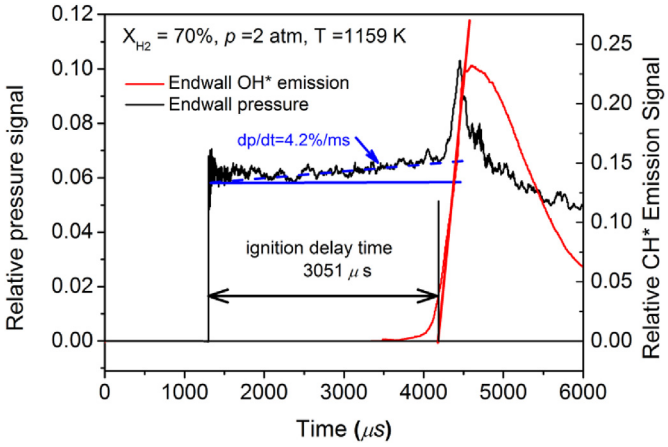

Fig. 1 – Determination of ignition delay time.

ideal effects during the experiments was considered in the simulation using the SENKIN/VTIM approach [44].

In this study, three representative kinetic mechanisms, namely the Pentane model [33,37,45], JetSurf model [46], and the LLNL model [47,48], were validated with experimental data. The Pentane model was optimized in 2015 by Curran and co-workers of NUI Galway based on their previous pentane isomer mechanism [45], which provides the low to high temperature kinetics of pentane. The rate coefficients of the C5 relevant reactions in this model were updated from several recent publications, besides, the thermodynamic parameters of C5 species were also reevaluated. Especially, the model was validated against the homogeneous ignition data from both the shock tube and rapid compression machine. JetSurf model was developed based on collaborative research by several universities with the support of the US Air Force [46]. It was developed to simulate the high temperature oxidation of *n*-alkanes up to C12 and high temperature kinetics of some cycloalkanes. LLNL model was developed to simulate the high and low temperature chemical kinetics of *n*-alkanes and 2-methyl alkanes, published by the Lawrence Livermore National Laboratory of the US [47,48]. Several versions of the detailed and skeletal mechanisms are provided for different simulation requirements. The detailed model suitable for the high temperature kinetics of *n*-alkanes up to C8 was employed here in this study.

Table 1 – Test mixture composition.

Mixture	Name	φ	X_{C5H12} (%)	X_{H2} (%)	X_{O2} (%)	X_{Ar} (%)
1. 100% H_2 [41]	H100	0.5	0	3.471	3.471	93.058
2. 95% H_2 5% C_5H_{12}	H95		0.107	2.036	3.75	94.107
3. 90% H_2 10% C_5H_{12}	H90		0.155	1.395	3.875	94.575
4. 70% H_2 30% C_5H_{12}	H70		0.221	0.515	4.046	95.218
5. 100% C_5H_{12}	H0		0.259	0	4.144	95.597

Results and discussions

Model validation

Firstly, the experimental results of individual fuels are compared with the simulations of different models, as shown in Fig. 2(1) and (2). For neat *n*-pentane (H0 mixture), given in Fig. 2(1), the predictions from the Pentane Model and JetSurf Model are quite close under the experimental pressures and all agree well with the ignition delay data. However, the LLNL Model overestimated the ignition delays of *n*-pentane under all the pressures. Meanwhile, it seems that such over-prediction tendency of the LLNL Model was more obvious at low pressures than that at high pressures, in other words, the deviation between model prediction and experimental data at 2 atm is greater than that at 20 atm. It is also found that among the above three models, the pressure-dependent rate constants of the unimolecular decomposition reactions of *n*-pentane were only considered in the recently published Pentane Model, by which the chemical kinetic of *n*-pentane is expected to be more reasonably interpreted.

The chemical kinetics of hydrogen always attracts much attention from researchers, there has been a lot of hydrogen ignition data available in literature [20,25,26,41,49]. In this study, previous data of hydrogen ignition from our group [41] were cited here for model evaluation. As shown in Fig. 2(2), among the three models, the predictions of the Pentane Model are in best agreement with the hydrogen ignition data under all the experimental pressures. Hydrogen sub-mechanism is usually the basis for the construction of kinetic models [50]. The chemical kinetics of the hydrogen subset in the JetSurf model is developed based on the GRI3.0 model [51] published in 1999, while that in the LLNL model is built based on the early work of Sarathy et al. [47,48] in 2011. Specifically, in the Pentane model, the hydrogen sub-mechanism has been updated based on the more recent experimental and theoretically studies of Hong et al. [52] and Nguyen et al. [53], the rate coefficients of some important reactions in hydrogen oxidation, such as $OH + HO_2 \Leftrightarrow H_2O + O_2$, $HO_2 + HO_2 \Leftrightarrow H_2O_2 + O_2$, $O + H_2O \Leftrightarrow OH + OH$ etc., were updated.

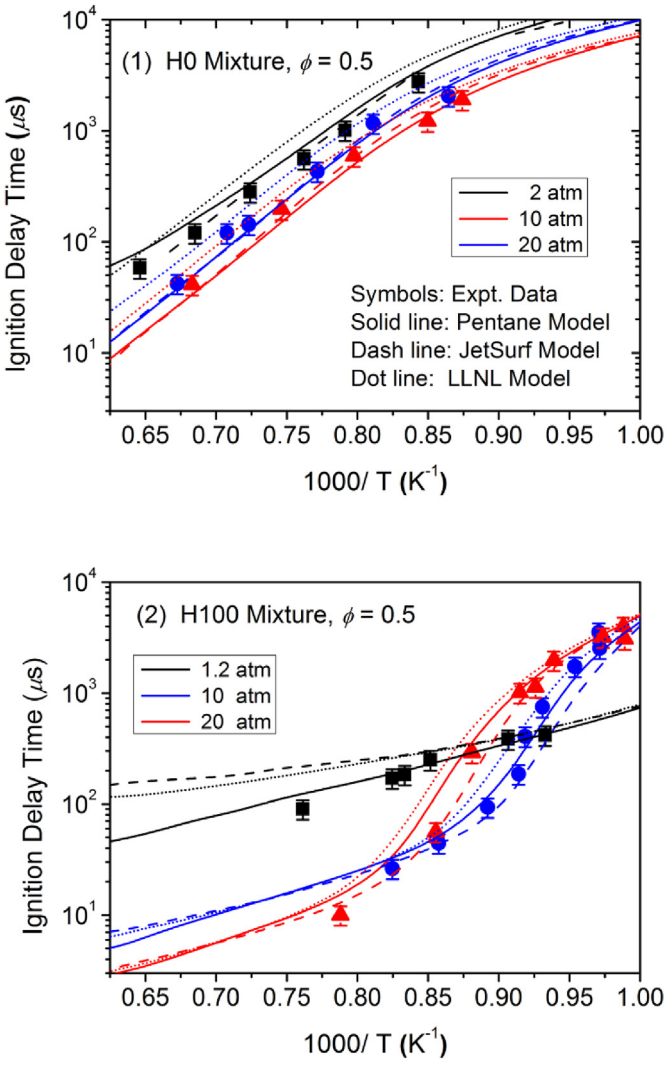

Fig. 2 – Comparisons between the measured and model-predicted ignition delay times of neat *n*-pentane and neat hydrogen (Hydrogen data were obtained from Ref. [41], using the same shock tube and fuel compositions as this study.).

Model validation of the hydrogen/*n*-pentane mixtures was also performed and it is found that the Pentane model can not only well predict the ignition delays of the individual fuels, but also well predict that of the binary mixtures, shown in Fig. 3. Generally, the Pentane model can well reproduce all the experimental data in this study. Besides, the chemical kinetics of both *n*-pentane and hydrogen in this model has been updated. Therefore, the Pentane model was selected to conduct simulation and kinetic analysis in this study.

Effect of pressure and empirical correlation

All the experimental data and simulation results in this study are shown in Fig. 3(1)–(5). Note that under all the experimental conditions, the ignition delay times of pure *n*-pentane and *n*-pentane/hydrogen mixtures always exhibit the typical Arrhenius dependence on the temperature. Therefore, the empirical correlations of the ignition delay times according to Eq. (1) is obtained and all the correlation parameters are given in Table 2

$$\tau = Ap^{\beta} \exp\left(\frac{E_a}{RT}\right) \quad (1)$$

where τ is ignition delay time, p is pressure, T is temperature, E_a is the activation energy, and R is the universal gas constant.

In the following, the effect of pressure on the ignition delay times of the dual-fuel mixture is discussed in view of different fuel blending ratios. Previous studies have demonstrated that the ignition delay times of neat hydrogen (H100 mixture) exhibit a non-monotonic pressure dependence with the change in temperatures [19,20,41], as shown in Fig. 3(5). That

Table 2 – Correlation of *n*-butane/hydrogen mixtures using Eq. (1).

Mixture	A	*b*	Ea (kcal/mol)	R^2
XH2 = 0%	2.12×10^{-4}	−0.337	39.10 ± 1.18	0.985
XH2 = 70%	8.40×10^{-4}	−0.450	35.84 ± 1.06	0.979
XH2 = 90%	1.32×10^{-4}	−0.459	38.99 ± 1.76	0.960
XH2 = 95%	5.05×10^{-4}	−0.412	34.44 ± 1.76	0.950

is, the ignition of hydrogen can be promoted with the increasing pressure only at relatively high temperatures, but inhibited by the rising pressures in the intermediate temperature regions. For neat *n*-pentane (H0 mixture), however, as shown in Fig. 3(1), the ignition delay times of *n*-pentane show the typical Arrhenius dependence on pressure and temperature which is similar to most alkanes.

It is worth noting that even just a small amount of *n*-pentane was added into hydrogen, namely 5% (H95 mixture), the hydrogen-like pressure dependence of ignition is replaced by the *n*-pentane-like behavior, in other words, the ignition delay times of the H95 mixture decrease monotonically as the pressure increases. Apparently, this alkane-like Arrhenius dependence was also observed for the H90 and H70 mixtures as *n*-pentane proportion increases.

Some literature have reported the hydrogen-like pressure dependence of hydrogen-enriched auto-ignition of *n*-alkanes. Zhang et al. [19] found the non-monotonic pressure-dependent characteristics of the 20%CH_4/80%H_2 mixtures during ignition, and this phenomenon disappears as the proportion of methane increases. In the experimental study of Man et al. [25], propane ignition gives the non-monotonic pressure dependence when the hydrogen ratio was as high as 95%. To further understand the transition of pressure dependence of hydrogen/*n*-alkane (C1–C5) binary mixtures, simulations were conducted using the Pentane Model at the equivalence of 0.5, pressures of 2 and 10 atm. During the simulation, hydrogen blending ratio was changed by 1% at a time to find out the minimum hydrogen percentage where the auto-ignition delay time at 2 and 10 atm start to present the non-monotonic pressure dependence. As clearly shown in Fig. 4 that, to behave the hydrogen-like non-monotonic pressure dependence, the longer the alkane carbon chain is, the larger hydrogen blending ratio is needed.

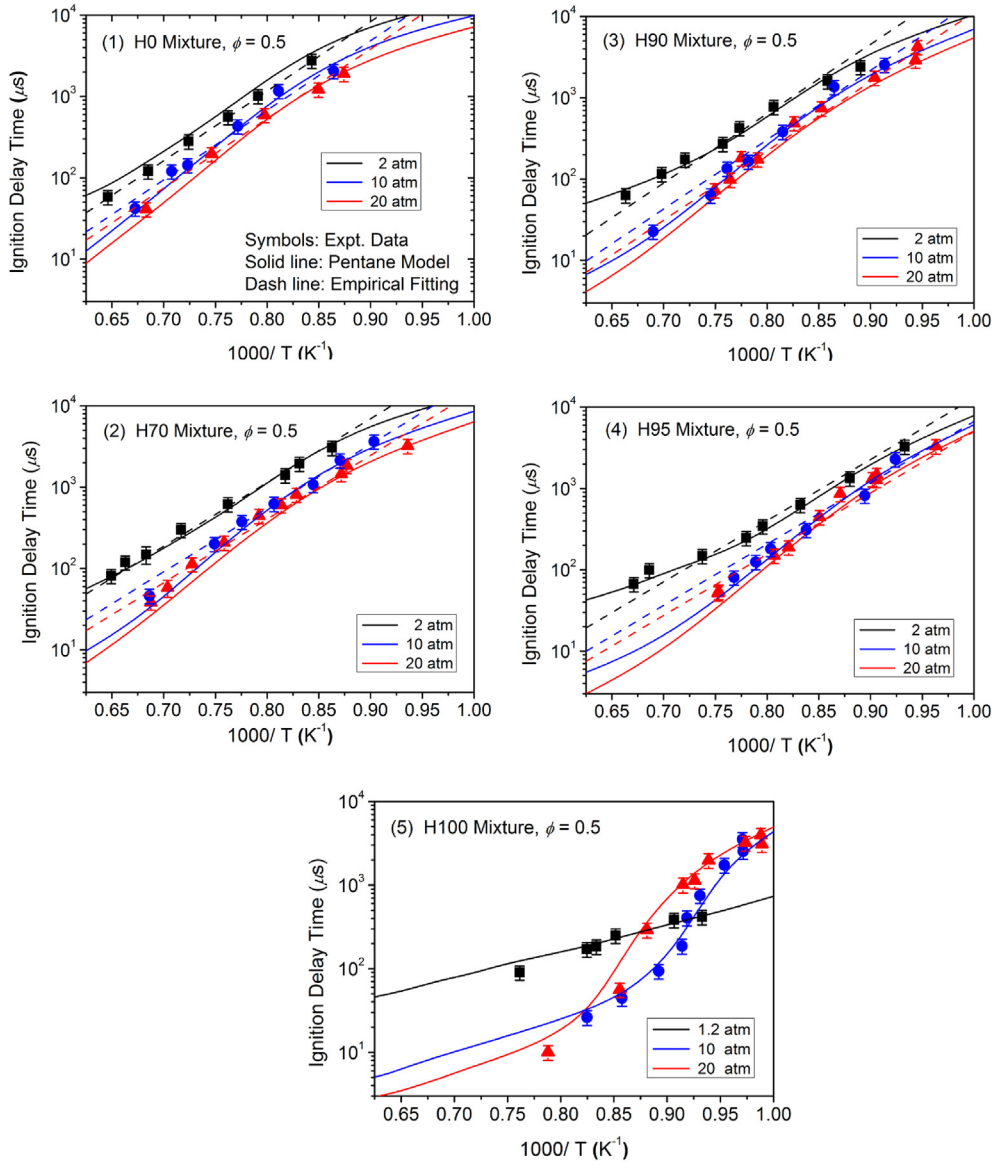

Fig. 3 – Effect of pressure on ignition delay times, comparison of the experimental results with the numerical results (Hydrogen data were obtained from Ref. [41]), and empirical fitting.

Effects of hydrogen blending

The ignition delay times of the lean hydrogen/*n*-pentane mixtures (H0 ~ H100) under different pressures, *i.e.* 2, 10, and 20 atm, together with the simulations with the Pentane Model are collectively shown in Fig. 5(1)–(3). Three observations can be readily observed.

First, the increase in hydrogen proportion in the hydrogen/*n*-pentane mixture lead to shorter ignition delay time, similar tendencies were observed under different pressures. Such a result is consistent with the literature studies of hydrogen-enriched ignition of C1–C4 *n*-alkanes [19,20,25–27]. The aforementioned information permits an initial inspection of the influence of hydrogen addition on the auto-ignitions of light *n*-alkanes, that is, hydrogen addition can always promote the ignition delays of C1–C5 straight-chain alkanes.

Second, the binary mixtures exhibit an *n*-pentane-like activation energy properties even if only a small amount of *n*-pentane (5%) is added. It is well known that the hydrogen presents obvious nonlinear combustion characteristic and segmented activation energies within different temperature regions, the transition in activation energies of hydrogen ignition can be seen clearly in Figs. 2 and 3. However, after the addition of 5% *n*-pentane, the ignition delay times under different pressures are all showing the typical Arrhenius dependence, similar to that of *n*-pentane.

Third, under the condition of different pressures, hydrogen addition always promotes the ignition delay time of *n*-pentane nonlinearly. A reduction factor $\Delta\tau$ is introduced in Fig. 6 to quantitatively describe the effect of hydrogen doping on the ignition delay time of *n*-pentane. $\Delta\tau$ is defined as:

$$\Delta\tau = \frac{\left(\tau_{X_{H2}} - \tau_{pentane}\right)}{\tau_{pentane}} \times 100\% \quad (2)$$

where, X_{H2} is the hydrogen blending ratio, $\tau_{X_{H2}}$ is the ignition delay time at the hydrogen blending ratio of X_{H2}, $\tau_{pentane}$ is the ignition delay time of pure *n*-pentane.

Fig. 6 shows the reduction factor of the *n*-pentane/hydrogen mixtures as a function of the hydrogen blending ratio at 20 atm. As shown in the figure, when the hydrogen ratio increases from 0% (H0) to 70% (H70), the changes of reduction factor $\Delta\tau$ are no more than 30% under different temperatures, this indicated that a presence of 70% hydrogen in the mixture can only decrease the ignition delay time by only less than 30% compare with the pure *n*-pentane. However, when further increases the hydrogen content form 70% (H70) to 90% (H90), the reduction factors under different temperatures all give the much sharper declines, indicating a more significant promotion effect of hydrogen on the ignition delay.

Chemical kinetic analyses

In order to further understand the observed experimental phenomena, chemical kinetic analyses were performed. The H radical consumption pathway of the H100 and H95 mixtures were analyzed in Fig. 7(1)–(3), at a pressure of 20 atm, equivalence ratio of 0.5, and temperatures of 1050 K, 1250 K, and 1425 K, respectively.

Experiments show that in the current conditions, in Fig. 3, the pure hydrogen gives a non-monotonic pressure dependence during ignition. This is mainly due to the competition between different depletion paths of H radical, in which the dominating channel varies as temperature and pressure changes [20]. Specifically speaking, the chain branching channel $H + O_2 \Leftrightarrow O + OH$ (R1) (promotes reactivity, high activation energy) is favored at high temperatures, the third-body recombination channels $H + O_2$ (+M) $\Leftrightarrow HO_2$ (+M) (R9) and $H + O_2$ (+AR) $\Leftrightarrow HO_2$ (+AR) (R10) (inhibit reactivity) are more favored at high pressures. The increase of pressure promotes the third-body reaction channel, at the same time, a decrease in temperature leads to relatively slow chain branching. As shown in Fig. 7(1)–(3), once $H + O_2$ (+M) $\Leftrightarrow HO_2$ (+M) (R9) and $H + O_2$ (+AR) $\Leftrightarrow HO_2$ (+AR) (R10) replace $H + O_2 \Leftrightarrow O + OH$ (R1) dominating the chemical kinetic during ignition, hydrogen shows the negative pressure dependence, which is the ignition delays become longer as pressure increases.

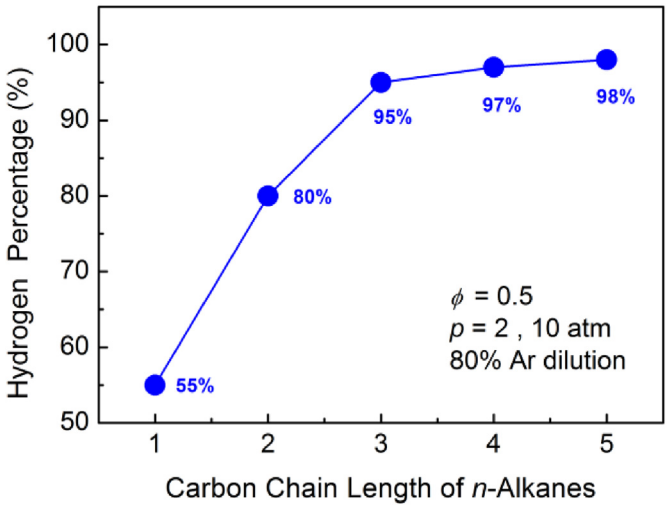

Fig. 4 – Minimum hydrogen percentage that the ignition delays of hydrogen/*n*-alkane (C1–C5) binary mixtures present the non-monotonic pressure dependence.

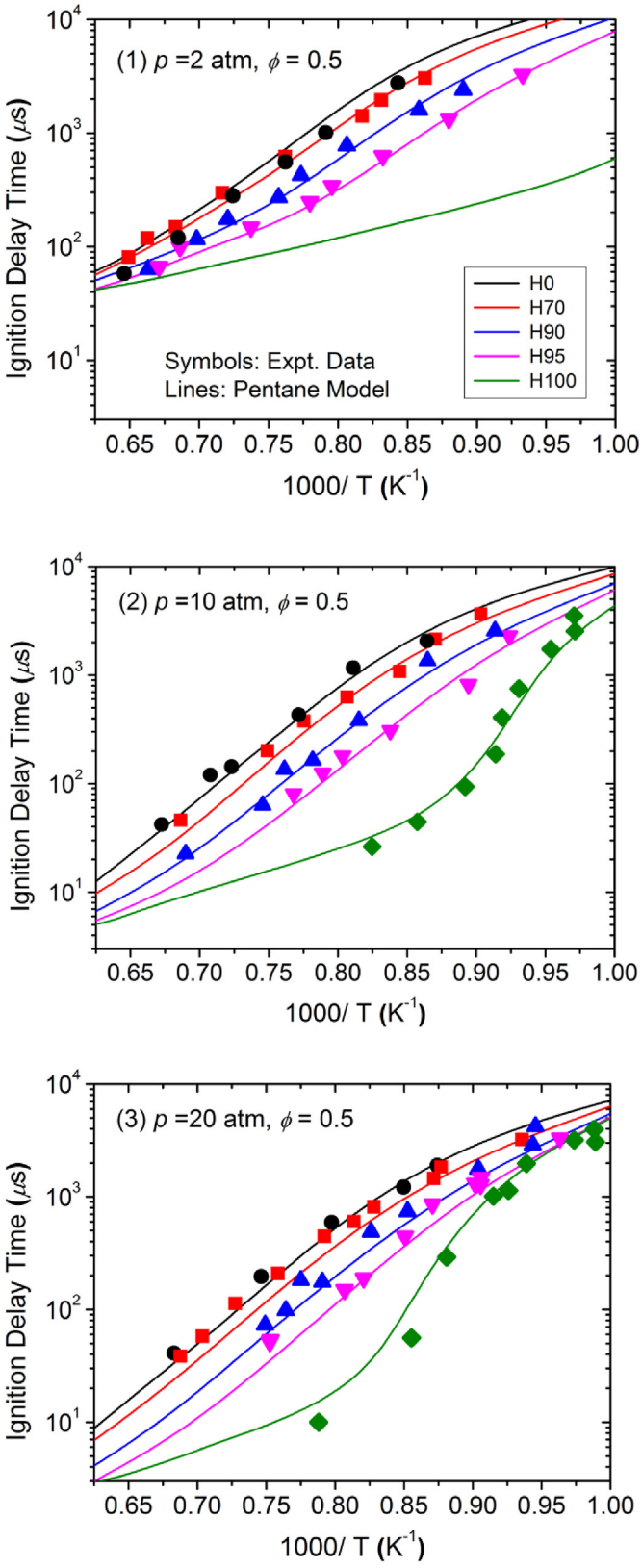

Fig. 5 – Experimental data and simulation of the ignition delay times of the lean ($\varphi = 0.5$) hydrogen/*n*-pentane mixtures under 2 atm, 10 atm and 20 atm (The pure hydrogen date are from literature [41])

For the H95 mixture, as shown in Fig. 7(2), in the temperature region where the negative pressure dependence of hydrogen occurred (1250 K), the addition of *n*-pentane lead to a considerable amount of H radical undergoes the *n*-pentane related pathway by $NC_5H_{12} + H \Leftrightarrow C_5H_11\text{-}1 + H_2$ (R2312), $NC_5H_{12} + H \Leftrightarrow C_5H_{11}\text{-}2 + H_2$ (R2313) and $NC_5H_{12} + H \Leftrightarrow C_5H_{11}\text{-}3 + H_2$ (R2314), but obviously weaken the paths of $H + O_2 \Leftrightarrow O + OH$ (R1), $H + O_2 (+M) \Leftrightarrow HO_2 (+M)$ (R9) and $H + O_2 (+AR) \Leftrightarrow HO_2 (+AR)$ (R10). The introduction of *n*-pentane into the chemical kinetic model diminished the competitive effect of hydrogen ignition between $H + O_2 \Leftrightarrow O + OH$ (R1) and $H + O_2 (+M) \Leftrightarrow HO_2 (+M)$ (R9), $H + O_2 (+AR) \Leftrightarrow HO_2 (+AR)$ (R10), eventually, the H95 fuel mixture gives the *n*-pentane-like pressure dependence. Compare with methane, larger alkanes, such as *n*-pentane, are more readily to react with H radicals due to their lower C–H bond energy and more C–H bonds in atoms, thus can affect the pressure dependent of hydrogen ignition under lower blending ratios.

Also note that after *n*-pentane addition, in Figs. 3 and 5, the piecewise activation energy of hydrogen ignition on temperature is replaced by the Arrhenius-like dependence. According to Fig. 7(1)–(3), under different temperatures, *n*-pentane addition always lead to the strong competition of H radical in the radical pool and resulting in the more pronounced H-abstraction pathways of *n*-pentane oxidation. For the H95 mixture, in the initial stages of ignition, the proportion of *n*-pentane H-abstraction pathways are approached or even exceed that of the hydrogen ignition pathway through $H + O_2 \Leftrightarrow O + OH$ (R1), $H + O_2 (+M) \Leftrightarrow HO_2 (+M)$ (R9) and $H + O_2 (+AR) \Leftrightarrow HO_2 (+AR)$ (R10). Therefore, a considerable amount of H radical consumed through the oxidation pathways of *n*-pentane rather than that of hydrogen during the ignition induction period, result in the pentane-like activation energy property of the binary mixtures.

According to Fig. 7, an increase in the proportion of hydrogen can decrease the ignition delay times of the binary fuel mixture not only since hydrogen itself is more reactive and ignite faster than *n*-pentane, in the meantime, more H radicals are involved with hydrogen blending which can also promote the H-abstraction of the *n*-pentane thus accelerate the process of *n*-pentane oxidation. As a result, the ignition *n*-pentane is promoted by hydrogen blending.

Fig. 8 shows the H radical rate of consumption as a function of hydrogen proportion in the initial stage of ignition. As can be seen, the consumption proportion of H radical through $H + O_2 \Leftrightarrow O + OH$ (R1) (chain branch reaction of hydrogen ignition) and that of $NC_5H_{12} + H \Leftrightarrow C_5H_11\text{-}1 + H_2$ (R2312), $NC_5H_{12} + H \Leftrightarrow C_5H_{11}\text{-}2 + H_2$ (R2313) and $NC_5H_{12} + H \Leftrightarrow C_5H_{11}\text{-}3 + H_2$ (R2314) (*n*-pentane H-abstraction pathways) were compared. Note that the nonlinearly variations of the H rate of consumption through the above reactions were observed with the increase of hydrogen blending ratio, which also corresponds to the nonlinear effect of hydrogen blending on the ignition delay of *n*-pentane in Fig. 5. As shown in Fig. 8, with 5% *n*-pentane addition, the proportion of $H + O_2 \Leftrightarrow O + OH$ (R1) pathway dropped sharply from 45.75% to 19.54%, at the same time, the proportion of H-abstractions through $NC_5H_{12} + H \Leftrightarrow C_5H_11\text{-}1 + H_2$ (R2312), $NC_5H_{12} + H \Leftrightarrow C_5H_{11}\text{-}2 + H_2$ (R2313) and $NC_5H_{12} + H \Leftrightarrow C_5H_{11}\text{-}3 + H_2$ (R2314) jumped from 0% to 57.72%. Meanwhile, when further increase the *n*-pentane proportion of the mixture, the changes in the consumption pathways become gentle. It is found that as the *n*-pentane increases from 5% to 100%, the branch of $H + O_2 \Leftrightarrow O + OH$ (R1) only decreases slightly from 19.54% to 11.57%.

Since the similar nonlinear promoting effect of hydrogen addition was observed in the high temperature auto-ignition of both *n*-butane [28] and *n*-pentane, Fig. 9 analyzed the peak mole fraction profiles of the H, O, and OH radicals as a function of hydrogen ratio for the *n*-butane/hydrogen and *n*-pentane/hydrogen mixtures at 1250 K, 20 atm and $X_{H2} = 0\%$–100%. The small radicals such as H, O, and OH are very reactive during the high temperature auto-ignition. They are important chain carries dominating the initiation, propagation, and termination of the elementary reactions, the concentration of which is closely related to the overall reactivity. It is found that the radical mole fraction profiles of the *n*-butane/hydrogen and *n*-pentane/hydrogen mixtures almost coincide at each hydrogen ratio. As shown in Fig. 9, the peak mole fractions of H, O, and OH radicals increased non-linearly with the increase of hydrogen blending ratio, this corresponds

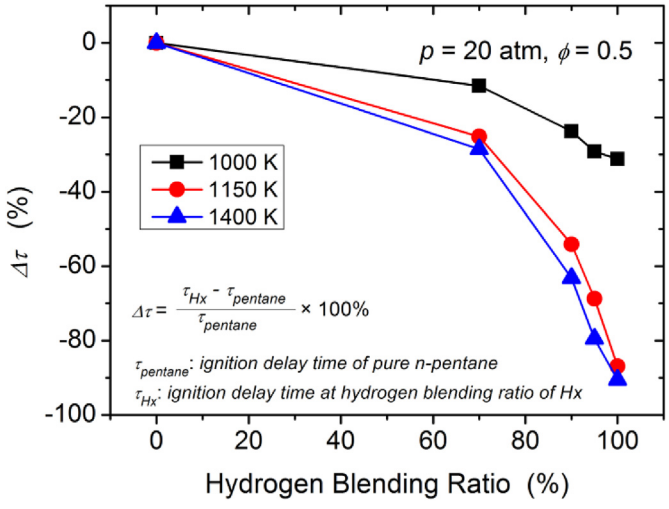

Fig. 6 – Effect of hydrogen blending ratio on the ignition delay times of *n*-pentane.

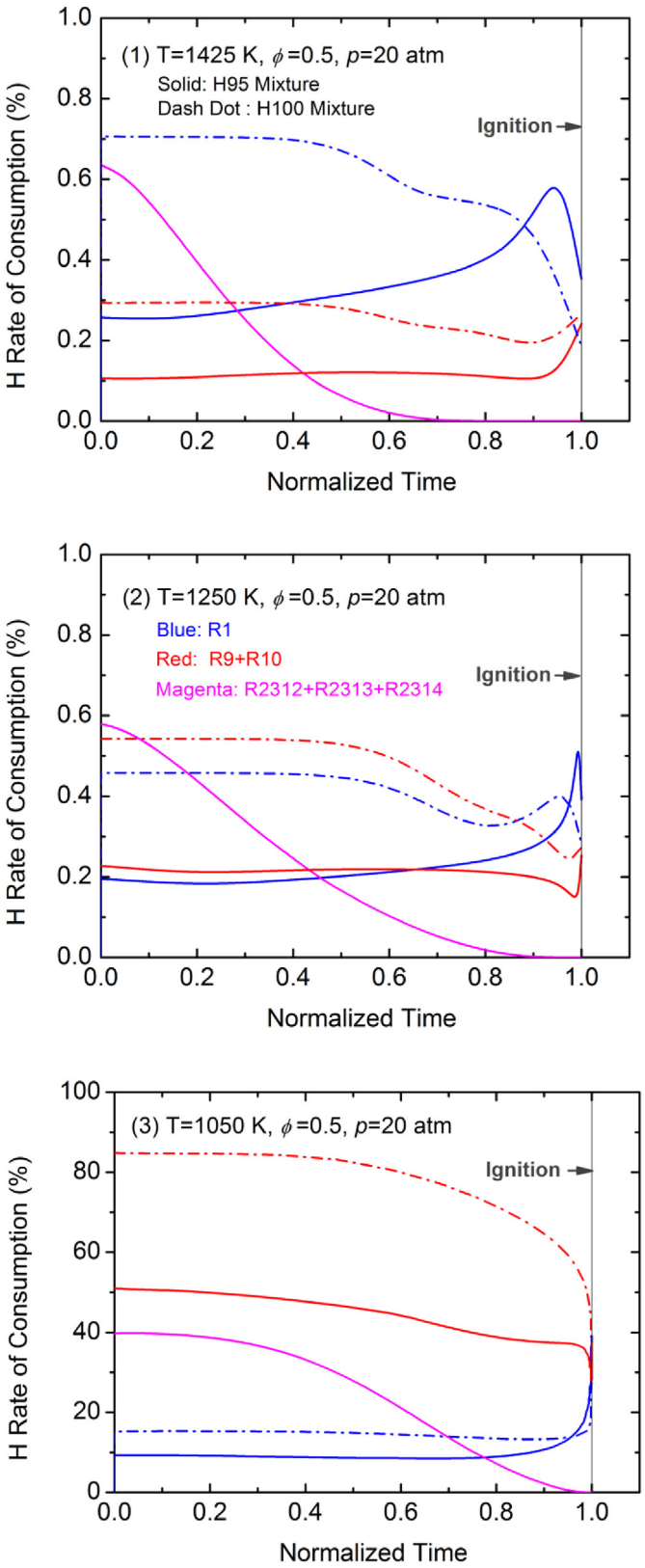

Fig. 7 – H radical rate of consumption as a function of normalized time (normalized time: the start time is zero and the moment of ignition is defined as one. Blue: $H + O_2 \Leftrightarrow O + OH$ (R1), Red: $H + O_2 (+M) \Leftrightarrow HO_2 (+M)$ (R9) and $H + O_2 (+AR) \Leftrightarrow HO_2 (+AR)$ (R10), Magenta: $NC_5H_{12} + H \Leftrightarrow C_5H_11\text{-}1 + H_2$ (R2312), $NC_5H_{12} + H \Leftrightarrow C_5H_{11}\text{-}2 + H_2$ (R2313), and $NC_5H_{12} + H \Leftrightarrow C_5H_{11}\text{-}3 + H_2$ (R2314)). (For interpretation of the references to colour in this figure legend, the reader is referred to the Web version of this article.)

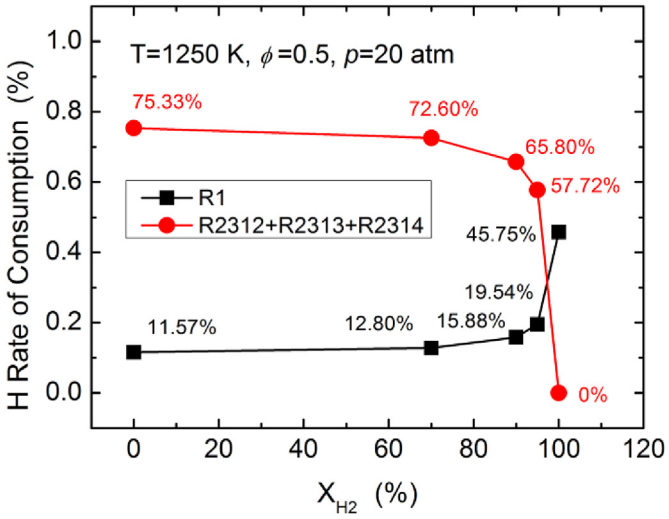

Fig. 8 – H radical rate of consumption in the initial stage of ignition as a function of hydrogen proportion.

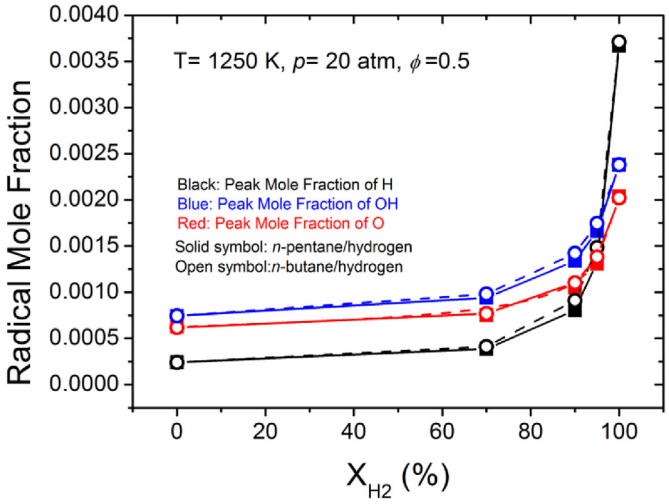

Fig. 9 – Peak mole fractions of H, O, and OH radicals as a function of hydrogen blending ratio during the ignition of *n*-butane/hydrogen and *n*-pentane/hydrogen mixtures.

to the ignition delay time profiles in Figs. 5 and 6. Note that relatively slow growths in the radical mole fractions were observed when the hydrogen blending ratio is smaller than 90%. However, once the hydrogen proportion exceeds 90%, the substantial growth of the radical concentrations appeared, indicating that active H, O, and OH radicals are produced to a large extent and promote the ignition.

Conclusion

The auto-ignition characteristic of lean (φ = 0.5) *n*-pentane/hydrogen mixture was experimentally investigated in a shock tube at pressures of 2, 10, and 20 atm, temperatures of 1038–1548 K. The main conclusions in this paper are as follows:

(1) The ignition delay times of the *n*-pentane/hydrogen blends (X_{H2} = 0, 70, 90, 95%) were measured. It is found that even only 5% *n*-pentane was blended into hydrogen, the binary mixtures exhibit the *n*-pentane-like activation energy properties and the ignition delay times satisfy the Arrhenius type dependence on temperature, empirical correlations of the ignition delay times are provided.

(2) The numerical simulations of the Pentane model, JetSurf model, and LLNL model were compared with the experimental data in this study. It is found that the Pentane model can well reproduce the ignition delay behavior of the *n*-pentane/hydrogen mixtures under the current conditions.

(3) Hydrogen addition can promote the ignition of *n*-pentane non-linearly, the ignition promotion effect is more significant at higher hydrogen ratios.

(4) Chemical kinetic analyses reveal that the H-abstraction reactions *n*-pentane has a strong ability to compete for H radicals with $H + O_2 \Leftrightarrow O + OH$ (R1), $H + O_2$ (+M) $\Leftrightarrow HO_2$ (+M) (R9), and $H + O_2$ (+AR) $\Leftrightarrow HO_2$ (+AR) (R10); therefore

make the kinetics of hydrogen less significant after blending. It is found that the peak mole fractions of the active free radicals, such as H, O, and OH, increased non-linearly with the increase of hydrogen blending ratio, this corresponds to the non-linearly promotion effect of hydrogen addition.

Declaration of competing interest

The authors declare that they have no known competing financial interests or personal relationships that could have appeared to influence the work reported in this paper.

Acknowledgements

This study is supported by the National Natural Science Foundation of China (NO. 51876164), China Postdoctoral Science Foundation Grant (2018M640987 and 2019T120907), State Key Laboratory of Engines, Tianjin University, and Jiangsu Province Key Laboratory of Aerospace Power System, China (CEPE2020009).

Appendix A. Supplementary data

Supplementary data to this article can be found online at https://doi.org/10.1016/j.ijhydene.2020.08.004.

REFERENCES

[1] Holladay JD, Hu J, King DL, Wang Y. An overview of hydrogen production technologies. Catal Today 2009;139(4):244–60. https://doi.org/10.1016/j.cattod.2008.08.039.
[2] Chiesa P, Lozza G, Mazzocchi L. Using hydrogen as gas turbine fuel. J Eng Gas Turbines Power 2005;127(1):163–71. https://doi.org/10.1115/1.1787513.
[3] Karim GA, Wierzba I, Al-Alousi Y. Methane-hydrogen mixtures as fuels. Int J Hydrogen Energy 1996;21(7):625–31. https://doi.org/10.1016/0360-3199(95)00134-4.
[4] Cheng RK, Oppenheim AK. Auto ignition in methane hydrogen mixtures. Combust Flame 1984;58(2):125–39. https://doi.org/10.1016/0010-2180(84)90088-9.
[5] Okafor EC, Hayakawa A, Nagano Y, Kitagawa T. Effects of hydrogen concentration on premixed laminar flames of hydrogen–methane–air. Int J Hydrogen Energy 2014;39(5):2409–17. https://doi.org/10.1016/j.ijhydene.2013.11.128.
[6] Hairuddin AA, Yusaf T, Wandel AP. A review of hydrogen and natural gas addition in diesel HCCI engines. Renew Sustain Energy Rev 2014;32:739–61. https://doi.org/10.1016/j.rser.2014.01.018.
[7] White CM, Steeper RR, Lutz AE. The hydrogen-fueled internal combustion engine: a technical review. Int J Hydrogen Energy 2006;31(10):1292–305. https://doi.org/10.1016/j.ijhydene.2005.12.001.
[8] Rozou S, Michaleas S, Antoniadou-Vyza E. Variable composition hydrogen/natural gas mixtures for increased engine efficiency and decreased emissions. J Eng Gas Turbines Power 2000;122(1):135–40. https://doi.org/10.1115/1.483191.
[9] Gökalp I, Lebas E. Alternative fuels for industrial gas turbines (AFTUR). Appl Therm Eng 2004;24(11–12):1655–63. https://doi.org/10.1016/j.applthermaleng.2003.10.035.
[10] Hu E, Huang Z, Zheng J, Li Q, He J. Numerical study on laminar burning velocity and NO formation of premixed methane–hydrogen–air flames. Int J Hydrogen Energy 2009;34(15):6545–57. https://doi.org/10.1016/j.ijhydene.2009.05.080.
[11] Coppens FHV, De Ruyck J, Konnov AA. Effects of hydrogen enrichment on adiabatic burning velocity and NO formation in methane/air flames. Exp Therm Fluid Sci 2007;31(5):437–44. https://doi.org/10.1016/j.expthermflusci.2006.04.012.
[12] Hu E, Huang Z, He J, Jin C, Zheng J. Experimental and numerical study on laminar burning characteristics of premixed methane–hydrogen–air flames. Int J Hydrogen Energy 2009;34(11):4876–88. https://doi.org/10.1016/j.ijhydene.2009.03.058.
[13] Amin V, Katzlinger G, Saxena P, Seshadri K. The influence of carbon monoxide and hydrogen on the structure and extinction of nonpremixed and premixed methane flames. Proc Combust Inst 2014;35(1):955–63. https://doi.org/10.1016/j.proci.2014.05.121.
[14] Konnov AA, Riemeijer R, De Goey LPH. Adiabatic laminar burning velocities of CH4/H2 air flames at low pressures. Fuel 2010;89(7):1392–6. https://doi.org/10.1016/j.fuel.2009.11.002.
[15] Brower M, Petersen EL, Metcalfe W, Curran H, Füri M, Bourque G, et al. Ignition delay time and laminar flame speed calculations for natural gas/hydrogen blends at elevated pressures. J Eng Gas Turbines Power 2013;135(2). https://doi.org/10.1115/1.4007763.
[16] Donohoe N, Heufer A, Metcalfe WK, Curran HJ, Davis ML, Mathieu O, et al. Ignition delay times, laminar flame speeds, and mechanism validation for natural gas/hydrogen blends at elevated pressures. Combust Flame 2014;161(6):1432–43. https://doi.org/10.1016/j.combustflame.2013.12.005.
[17] Dagaut P, Nicolle A. Experimental and detailed kinetic modeling study of hydrogen-enriched natural gas blend oxidation over extended temperature and equivalence ratio ranges. Proc Combust Inst 2005;30(2):2631–8. https://doi.org/10.1016/j.proci.2004.07.030.
[18] Dagaut P, Dayma G. Hydrogen-enriched natural gas blend oxidation under high-pressure conditions: experimental and detailed chemical kinetic modeling. Int J Hydrogen Energy 2006;31(4):505–15. https://doi.org/10.1016/j.ijhydene.2005.04.020.
[19] Zhang Y, Huang Z, Wei L, Zhang J, Law CK. Experimental and modeling study on ignition delays of lean mixtures of methane, hydrogen, oxygen, and argon at elevated pressures. Combust Flame 2012;159(3):918–31. https://doi.org/10.1016/j.combustflame.2011.09.010.
[20] Herzler J, Naumann C. Shock-tube study of the ignition of methane/ethane/hydrogen mixtures with hydrogen contents from 0% to 100% at different pressures. Proc Combust Inst 2009;32(1):213–20. https://doi.org/10.1016/j.proci.2008.07.034.
[21] Chaumeix N, Pichon S, Lafosse F, Paillard CE. Role of chemical kinetics on the detonation properties of hydrogen/natural gas/air mixtures. Int J Hydrogen Energy 2007;32(13):2216–26. https://doi.org/10.1016/j.ijhydene.2007.04.008.
[22] Huang J, Bushe WK, Hill PG, Munshi SR. Experimental and kinetic study of shock initiated ignition in homogeneous methane–hydrogen–air mixtures at engine-relevant conditions. Int J Chem Kinet 2006;38(4):221–33. https://doi.org/10.1002/kin.20157.

[23] Gersen S, Anikin NB, Mokhov AV, Levinsky HB. Ignition properties of methane/hydrogen mixtures in a rapid compression machine. Int J Hydrogen Energy 2008;33(7):1957–64. https://doi.org/10.1016/j.ijhydene.2008.01.017.
[24] Yu Y, Vanhove G, Griffiths JF, De Ferrières S, Pauwels JF. Influence of EGR and syngas components on the autoignition of natural gas in a rapid compression machine: a detailed experimental study. Energy Fuel 2013;27(7):3988–96. https://doi.org/10.1021/ef400336x.
[25] Man X, Tang C, Wei L, Pan L, Huang Z. Measurements and kinetic study on ignition delay times of propane/hydrogen in argon diluted oxygen. Int J Hydrogen Energy 2013;38(5):2523–30. https://doi.org/10.1016/j.ijhydene.2012.12.020.
[26] Tang C, Man X, Wei L, Pan L, Huang Z. Further study on the ignition delay times of propane-hydrogen-oxygen- argon mixtures: effect of equivalence ratio. Combust Flame 2013;160(11):2283–90. https://doi.org/10.1016/j.combustflame.2013.05.012.
[27] Jiang X, Pan Y, Sun W, Liu Y, Huang Z. Shock-tube study of the autoignition of n-butane/hydrogen mixtures. Energy Fuel 2018;32(1):809–21. https://doi.org/10.1021/acs.energyfuels.7b02423.
[28] Jiang X, Pan Y, Liu Y, Sun W, Huang Z. Experimental and kinetic study on ignition delay times of lean n-butane/hydrogen/argon mixtures at elevated pressures. Int J Hydrogen Energy 2017;42(17):12645–56. https://doi.org/10.1016/j.ijhydene.2017.03.196.
[29] Pan L, Zhang Y, Zhang J, Tian Z, Huang Z. Shock tube and kinetic study of C 2 H 6/H 2/O 2/Ar mixtures at elevated pressures. Int J Hydrogen Energy 2014;39(11):6024–33. https://doi.org/10.1016/j.ijhydene.2014.01.157.
[30] Leppard WR, Rapp LA, Burns VR, Gorse RA, Knepper JC, Koehl WJ. Effects of gasoline composition on vehicle engine-out and tailpipe hydrocarbon emissions - the auto/oil air quality improvement research program. SAE paper. 1992. https://doi.org/10.4271/920329.
[31] Westbrook CK, Curran HJ, Pitz WJ, Griffiths JF, Mohamed C, Wo SK. The effects of pressure, temperature, and concentration on the reactivity of alkanes: experiments and modeling in a rapid compression machine. Sympo Comb 1998;27(1):371–8. https://10.1016/S0082-0784(98)80425-6.
[32] Zhukov VP, Sechenov VA, Starikovskii AY. Self-ignition of a lean mixture of n -pentane and air over a wide range of pressures. Combust Flame 2005;140(3):196–203. https://doi.org/10.1016/j.combustflame.2004.11.008.
[33] Bugler J, Marks B, Mathieu O, Archuleta R, Camou A, Grégoire C, et al. An ignition delay time and chemical kinetic modeling study of the pentane isomers. Combust Flame 2016;163:138–56. https://doi.org/10.1016/j.combustflame.2015.09.014.
[34] Kelley AP, Smallbone AJ, Zhu DL, Law CK. Laminar flame speeds of C5 to C8 n-alkanes at elevated pressures: experimental determination, fuel similarity, and stretch sensitivity. Proc Combust Inst 2011;33(1):963–70. https://doi.org/10.1016/j.proci.2010.06.074.
[35] Cheng Y, Hu E, Lu X, Gong J, Li Q, Huang Z. Experimental and kinetic study of pentene isomers and n-pentane in laminar flames. Proc Combust Inst 2017;36(1):1279–86. https://doi.org/10.1016/j.proci.2016.08.026.
[36] Ji C, Dames E, Wang YL, Wang H, Egolfopoulos FN. Propagation and extinction of premixed C5–C12 n-alkane flames. Combust Flame 2010;157(2):277–87. https://doi.org/10.1016/j.combustflame.2009.06.011.
[37] Bugler J, Rodriguez A, Herbinet O, Battin-Leclerc F, Togbé C, Dayma G, et al. An experimental and modelling study of n-pentane oxidation in two jet-stirred reactors: the importance of pressure-dependent kinetics and new reaction pathways. Proc Combust Inst 2017;36(1):441–8. https://doi.org/10.1016/j.proci.2016.05.048.
[38] Rodriguez A, Herbinet O, Wang Z, Qi F, Fittschen C, Westmoreland PR, et al. Measuring hydroperoxide chain-branching agents during n-pentane low-temperature oxidation. Proc Combust Inst 2017;36(1):333–42. https://doi.org/10.1016/j.proci.2016.05.044.
[39] Jiang X, Zhang Y, Man X, Pan L, Huang Z. Shock tube measurements and kinetic study on ignition delay times of lean DME/n-butane blends at elevated pressures. Energy Fuel 2013;27(10):6238–46. https://doi.org/10.1021/ef401252e.
[40] Jiang X, Zhang Y, Man X, Pan L, Huang Z. Experimental and modeling study on ignition delay times of dimethyl ether/n-butane blends at a pressure of 2.0 MPa. Energy Fuel 2014;28(3):2189–98. https://doi.org/10.1021/ef402277h.
[41] Lun P, Hu E, Deng F, Zhang Z, Huang Z. Effect of pressure and equivalence ratio on the ignition characteristics of dimethyl ether-hydrogen mixtures. Int J Hydrogen Energy 2014;39(33):19212–23. https://doi.org/10.1016/j.ijhydene.2014.09.098.
[42] Lutz AE, Kee RJ, Miller JA. SENKIN: a sensitivity, for predicting homogeneous gas analysis. Livermore, CA: Sandia National Laboratories; 1988. https://www.osti.gov/biblio/5371815. [Accessed 16 July 2020].
[43] Kee RJ, Rupley FM, Miller JA. CHEMKIN-II: a chemical, chemical kinetics package for kinetics. Livermore, CA: Sandia National Laboratories; 1989. https://www.osti.gov/biblio/5681118. [Accessed 16 July 2020].
[44] Chaos M, Dryer FL. Chemical-kinetic modeling of ignition delay: considerations in interpreting shock tube data. Int J Chem Kinet 2010;42(3):143–50. https://doi.org/10.1002/kin.20471.
[45] Bugler J, Somers KP, Silke EJ, Curran HJ. Revisiting the kinetics and thermodynamics of the low-temperature oxidation pathways of alkanes: a case study of the three pentane isomers. J Phys Chem 2015;119(28):7510–27. https://doi.org/10.1021/acs.jpca.5b00837.
[46] Wang H, Dames E, Sirjean B, Sheen DA, Tango R, Violi A, et al. A high-temperature chemical kinetic model of n-alkane (up to n-dodecane), cyclohexane, and methyl-, ethyl-, n-propyl and n-butyl-cyclohexane oxidation at high temperatures. 2010. JetSurF version 2.0, http://web.stanford.edu/group/haiwanglab/JetSurF/JetSurF2.0/index.html.
[47] Sarathy SM, Westbrook CK, Mehl M, Pitz WJ, Togbe C, Dagaut P, et al. Comprehensive chemical kinetic modeling of the oxidation of 2-methylalkanes from C7 to C20. Combust Flame 2011;158(12):2338–57. https://doi.org/10.1016/j.combustflame.2011.05.007.
[48] Sarathy SM, Yeung C, Westbrook CK, Pitz WJ, Meh M, Thomson MJ. An experimental and kinetic modeling study of n-octane and 2-methylheptane in an opposed-flow diffusion flame. Combust Flame 2011;158(7):1277–87. https://doi.org/10.1016/j.combustflame.2010.11.008.
[49] Pang GA, Davidson DF, Hanson RK. Experimental study and modeling of shock tube ignition delay times for hydrogen–oxygen–argon mixtures at low temperatures. Proc Combust Inst 2009;32(1):181–8. https://doi.org/10.1016/j.proci.2008.06.014.

[50] Karim GA, Wierzba I, Al-Alousi Y. Methane-hydrogen mixtures as fuels. Int J Hydrogen Energy 1996;21(7):625–31. https://doi.org/10.1016/0360-3199(95)00134-4.
[51] Smith G, Golden D M, Frenklach M, Frenklach M, Moriarty NW, Eiteneer B, et al. GRI-Mech 3.0. 1999. http://combustion.berkeley.edu/gri-mech/. [Accessed 16 July 2020].
[52] Hong Z, Lam KY, Sur R, Wang S, Davidson DF, Hanson RK. On the rate constants of OH + HO 2 and HO2 + HO2 : a comprehensive study of H2O2 thermal decomposition using multi-species laser absorption. Proc Combust Inst 2013;34(1):565–71. https://doi.org/10.1016/j.proci.2012.06.108.
[53] Nguyen TL, Stanton JF. Ab initio thermal rate calculations of HO + HO = O(3P) + H2O reaction and isotopologues. J Phys Chem 2013;117(13):2678. https://doi.org/10.1021/jp312246q.